Molecular Therapy
Nucleic Acids
Original Article

Enhancing MicroRNA Activity through Increased Endosomal Release Mediated by Nigericin

Esteban A. Orellana,[1,4] Ahmed M. Abdelaal,[1] Loganathan Rangasamy,[2] Srinivasarao Tenneti,[2,5] Sunghyun Myoung,[1] Philip S. Low,[2,3] and Andrea L. Kasinski[1,3]

[1]Department of Biological Sciences, Purdue University, West Lafayette, IN 47907, USA; [2]Department of Chemistry, Purdue University, West Lafayette, IN 47907, USA; [3]Purdue Center for Cancer Research, Purdue University, West Lafayette, IN 47907, USA

The therapeutic promise of small-RNA therapeutics is limited, not only by the lack of delivery vehicles, but also by the inability of the small RNAs to reach intracellular compartments where they can be biologically active. We previously reported successful delivery of functionally active miRNAs via receptor-mediated endocytosis. This type of targeted therapy still faces a major challenge in the delivery field: endosomal sequestration. Here, a new method has been developed to promote endosomal escape of delivered miRNA. The strategy relies on the difference in solute contents between nascent endosomes and the cytoplasm; early endosomes are rich in sodium ions, whereas the intracellular fluid is rich is potassium ions. Exploiting this difference through favoring the influx of potassium into the endosomes without the exchange of osmotically active sodium, results in an osmotic differential leading to the endosomes swelling and bursting. One molecule that is able to exchange potassium for an osmotically inactive hydrogen ion is the ionophore nigericin. Through generating an intramolecular miRNA delivery vehicle, containing a ligand, in this case folate and nigericin, we enabled the escape of folate-RNA conjugates from their entrapping endosomes into the cytoplasm where they bound the RNA-induced silencing complex and activated the RNAi response.

INTRODUCTION

The therapeutic prospect of miRNA replacement therapies relies on reintroducing small, synthetic RNA molecules that mimic endogenous miRNAs in cells that have lost them, with the final goal of restoring cellular pathways that could stop pathogenesis.[1–3] However, a major constraint in the transition of miRNA mimics, and other small RNAs (small interfering RNA [siRNA]; antisense oligonucleotides), into the clinic has been the lack of efficient delivery systems. Encapsulation of small RNAs, for instance, has had mixed results in the clinic with clinical trials showing toxicity and limited efficacy.[4] Some problems that come with the use of encapsulating delivery vehicles (e.g., liposomes, micelles, and polymers) include delivery-associated toxicity, poor transfection efficiency, and nonspecific biodistribution.[5]

Our previous work showed that these vehicle-related defects may be overcome by eliminating the vehicle, attaching a miRNA to a folate ligand (FolamiR).[6] This approach can deliver functionally active miRNAs to cancer cells that overexpress the folate receptor (FR) via receptor-mediated endocytosis with no signs of toxicity (maximum tolerated dose, >26.64 mg/kg).[6] Thus, in the absence of toxicity, the main factors limiting dosage would be two-fold: (1) the internalization kinetics of the folate-ligand bound to its receptor (endocytosis) and (2) the rate at which the FolamiR can escape the endosome.[7,8]

We reasoned that, since the internalization kinetics of FolamiRs are less amendable and already rapid,[9–11] the development and inclusion of an endosomal escape mechanism onto next-generation FolamiRs could help overcome the rate-limiting step of endosomal escape, providing higher efficacy and further reducing toxicity. The endosomal escape of small RNAs (and other biologics) has been recognized as a major hindrance in the path to translating RNA therapeutics into the clinic. For that reason efforts have been focused on developing strategies to enhance endosomal release and secure cytosolic delivery.[12] Proteins and peptide-based agents (i.e., cell-penetrating peptides [CPPs]) are often used to achieve cytosolic release of oligonucleotides.[12] For instance, the EB1 peptide, derived from penetratin is a CPP with endosomolytic properties that facilitate transport of active siRNAs into cells.[13] Similarly, the inclusion of the influenza-derived fusogenic peptide diINF-7 has been shown to enhance endosomal escape of siRNAs when complexed with lipid carriers.[14] However, the use of peptides is often toxic and may contribute to increased immunogenicity,[15] which is already a major concern in RNA therapeutics. Another approach to improving endosomal release of nucleic acids is the use of "proton sponges" that can promote endosomal swelling by inducing counterion uptake that leads to increased osmotic pressure.[16] The practicality of using this strategy in the clinic is dampened by the large concentration of compound needed to achieve efficient endosomal bursting.[16] Photochemical

Received 11 July 2018; accepted 6 April 2019;
https://doi.org/10.1016/j.omtn.2019.04.003.

[4]Present address: Stem Cell Program, Boston Children's Hospital, Harvard Medical School, Boston, MA 02115, USA

[5]Present address: Department of Chemistry and Biochemistry, Ohio State University, Columbus, OH 43202, USA

Correspondence: Andrea L. Kasinski, MD, Department of Biological Sciences, Purdue University, West Lafayette, IN 47907, USA.
E-mail: akasinski@purdue.edu

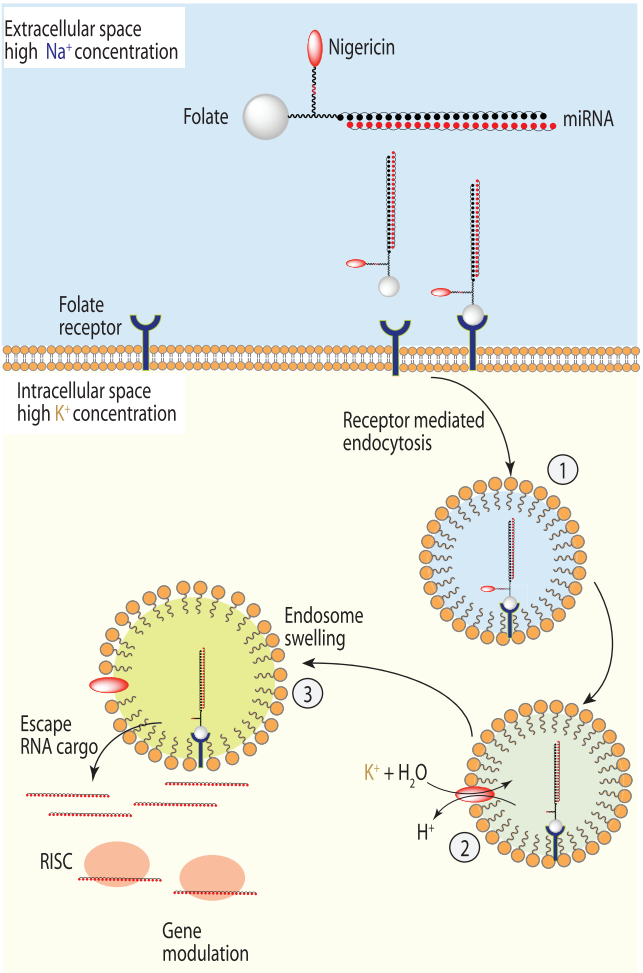

Figure 1. Proposed Mechanism of Action of Endosomal Escape of RNA Cargo Mediated by Ligand-Targeted Delivery of Nigericin

Internalization of folate-nigericin-RNA (Fol-Nig-RNA) conjugates is mediated by endocytosis. (1) The nascent vesicle is rich in extracellular fluid with a high concentration of Na^+ (blue shading), whereas the intracellular space contains high levels of K^+ (yellow shading). (2) Upon ligand-targeted delivery, nigericin, a K^+/H^+ antiporter, translocates to the endosomal membrane (following reduction of the di-sulfide bond, red linker) causing an influx of K^+ (green shading) in exchange for H^+. (3) The exchange of K^+ for the osmotically inactive H^+ leads to buildup of osmotic pressure, which causes endosomal swelling and release of RNA cargo into the cytosol.

internalization (PCI) is another alternative to increase endosomal escape of siRNAs, but this approach is greatly limited to specific sites where light can be used to trigger endosome lysis, which reduces its practical use in the clinic.[17]

We recently described a novel method of facilitating the escape of biologics from entrapping endosomes and, in that study, provided preliminary evidence for the potential use of this method to improve the escape of small RNAs from endosomes.[18] The strategy relies on the difference in solute contents between nascent endosomes and the cytoplasm; endosomes are rich in sodium ions (Na^+), whereas the intracellular fluid is rich is potassium ions (K^+). The method exploits this difference by using a small molecule, nigericin,[19,20] that exchanges K^+ for an osmotically inactive proton (H^+) to achieve a balance in charge without release of a compensatory solute (Na^+), thus causing an osmotic differential that leads to endosome swelling and bursting.[18]

Herein, we show that this approach is useful in overcoming endosomal entrapment of small RNAs delivered by folate. The data presented here suggest that ligand-targeted delivery of nigericin into endosomes can facilitate the escape of RNA cargo (e.g., miRNAs, siRNAs) from their entrapping endosomes, helping the small RNAs to become available in the cytoplasm, engage the RNA-induced silencing complex (RISC) and improve their RNAi activity (see proposed model in Figure 1). Developing a highly specific delivery platform (i.e., FolamiRs) with increased endosomolytic properties could be useful in achieving significant therapeutic effects of therapeutic miRNAs at low concentrations without unwanted toxicity for future *in vivo* applications.

RESULTS

Evidence of Endosomal Entrapment of Folate-miRNA Conjugates

We previously reported that miRNAs conjugated to folate retain their activity in cells in culture and *in vivo*, suggesting that some of the delivered miRNA is available in the cytosol for loading into the RISC. Regardless, receptor-mediated endocytosis is a well-documented mechanism for uptake of ligand conjugates that interact with cell surface receptors. To determine if folate conjugates are sequestered within the endosomes, confocal imaging of cells was performed after treatment of cells with folate cyanine 5 (Cy5). As indicated in Figure 2A, defined punctate spots were observed, some of which co-localized with the early endosome marker Rab5.[21] To determine if entrapment of FolamiR-34a in the endosomes is a rate-limiting effect that reduces the overall activity of the miRNA, FolamiR-34a-treated cells were exposed to chloroquine, which causes protonation in acidic environments of the late endosomes. Protonation results in H^+, Cl^-, and water entering into the endosome, resulting in osmotic swelling and eventual rupture.[12] miRNA activity in the presence and absence of chloroquine was monitored using a miR-34a sensor stably integrated into the genome of the FR-positive (FR^+) cell line, MB-231. The sensor contains a miR-34a binding site downstream of luciferase, resulting in luciferase repression in the presence of active miR-34a. Twenty-four hours after administering FolamiR-34a, minimal reporter silencing was observed, as we have previously reported at this early time point[6] (Figure 2B). However, in the presence of chloroquine, silencing of the miR-34a reporter was more robust, resulting in ~40% reduction in luciferase activity. Collectively, these data suggest that folate-miRNA conjugates are taken up via the process of receptor-mediated endocytosis and that some of the miRNA remains entrapped within the endosome. Thus, endosomal escape of FolamiRs is a major limitation to achieving robust miRNA activity.

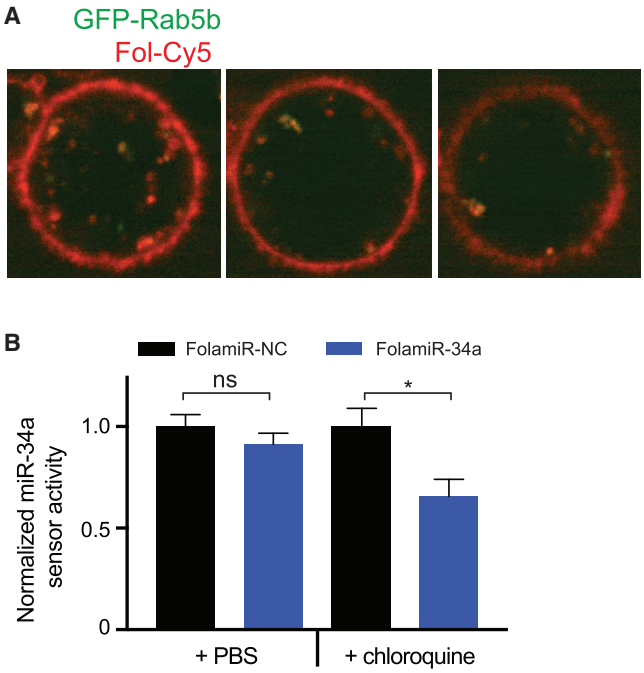

Figure 2. Sequestration of Folate Conjugates Inside the Endosome

(A) MB-231 FR$^+$ cells transiently expressing the early endocytic marker GFP-Rab5b were treated with Fol-Cy5. Confocal images were acquired 30 min after treatment. Three representative images are shown. (B) MB-231 FR$^+$ miR-34a sensor cells were treated with folate conjugates, followed 4 h later by treatment with 10 μM chloroquine. After 48 h, sensor activity was measured. The experiment corresponds to three biological replicates with at least three technical replicates per treatment (error bars: mean ± SD; *$p < 0.05$, one-way ANOVA with post hoc Bonferroni correction). FolamiR-NC: folate conjugated to a negative control RNA

Folate-Nigericin-miRNA Conjugation and Stability in Serum

We reasoned that intramolecular inclusion of a small molecule that can facilitate endosomal escape of the folate-conjugated miRNA will enhance the cytosolic distribution and activity of the miRNA. To address this possibility, the small-molecule ionophore nigericin was conjugated to the folate-miRNA conjugate. Since nigericin needs to dissociate from the folate carrier and localize to the endosomal membrane to induce endosome swelling (exchanging intracellular K^+ for endosomal H^+), an intramolecular disulfide linkage was incorporated between nigericin and the folate-RNA conjugate (Figure 3A). Folate-nigericin-miRNA conjugation was achieved as previously described[6] by using click chemistry,[22] and conjugation was verified by PAGE analysis (Figure 3B) and MALDI spectral analysis (not shown). Disulfide linkage reduction was verified by PAGE analysis by a band-size shift after tris(2- carboxyethyl)phosphine (TCEP) treatment (Figure 3B, lane 4). To test the stability of the disulfide linkage, FolamiR-34a, with an intramolecular conjugation to nigericin (Fol-Nig-34a), was exposed to 50% serum. There were no signs of Fol-Nig-34a reduction for 4 h (Figure 3C), leaving open the possibility that premature reduction upon systemic delivery could occur after 4 h. Our previous results using FolamiRs *in vivo* determined that less than 4 h is enough time for the folate conjugates to localize and be internalized into the intended tissues.[6]

Folate-Nigericin-miRNA Conjugate Uptake Is Mediated by the Folate Receptor

Because of the high affinity of the ionophore nigericin for cellular membranes, it was important to verify that uptake of folate-nigericin-miRNA (Fol-Nig-miRNA) conjugates is mediated by the FR. For that purpose, expression of the FR in MB-231 cells and KB cells was verified by flow cytometric analyses, as previously reported,[6,23] using Fol-Cy5 (Figure 4A). Next, to visualize cellular uptake of miR-34a in the absence or presence of nigericin, an Atto-647N fluorophore was attached to the 5′ end of the miR-34a-5p strand generating Fol-34a-Atto647N and Fol-Nig-34a-Atto647N. The specificity of cellular uptake of Fol-34a-Atto647N and Fol-Nig-34a-Atto647N conjugates was determined in the presence or absence of folate-glucosamine as a competitor (Figures 4B and 4C). Both conjugates were taken up by MB-231 and KB cells, only in the absence of folate-glucosamine, suggesting that the uptake is FR mediated. Furthermore, minimal uptake in the absence of folate conjugation (gymnotic uptake) was observed (Figure 4D; duplex miR-34a-Atto647N). Taken together, these results suggest that Fol-Nig-miRNA uptake is mediated by the FR.

Ligand-Targeted Delivery of Nigericin Causes Endosomal Release of miR-34a

To track the release of cargo from endosomes, Cy5 was delivered with either a folate-only or a folate-nigericin carrier, and the fluorescent cellular distribution was used as a surrogate for cargo localization. For that purpose, FR$^+$ MB-231 cells were incubated with 50 nM of Fol-Cy5 or Fol-Nig-Cy5 and imaged every 2 min over the course of 1 h. Representative images of the cells at 15 min after treatment are presented in Figure 5A. The intracellular distribution of Cy5 was noticeably different in the absence of nigericin. Cells treated with Fol-Cy5 showed fluorescent signal in the cell membrane and individual punctate spots throughout the cytoplasm, indicative of endosomal localization.[11] In contrast, cells treated with Fol-Nig-Cy5 showed perinuclear distribution as string-like dispersions with fewer clearly distinguishable punctate spots and more diffuse cytoplasmic localization.

Next, to monitor the localization of miR-34a delivered via folate conjugation in the absence or presence of nigericin, FR$^+$ KB cells were incubated with 50 nM of Fol-34a-Atto647N or Fol-Nig-34a-Atto647N and imaged every 2 min for 3 h. As early as 30 min after treatment, noticeably larger vesicles were observed in the cells treated with Fol-Nig-34a-Atto647N conjugate, compared with the vesicles of cells treated with Fol-34a-Atto647N (Figure 5B, quantified in Figure 5C). Interestingly, the total number of fluorescent punctate spots detected in cells treated with Fol-Nig-34a-Atto647N was reduced compared with those in cells treated with Fol-34a-Atto647N (Figure 5D), which could suggest that miR-34a-Atto647N delivered with the folate-nigericin carrier is not entrapped within the endosomes and that the larger size of the fewer vesicles is indicative of endosomal swelling. Taken together, these data suggest that

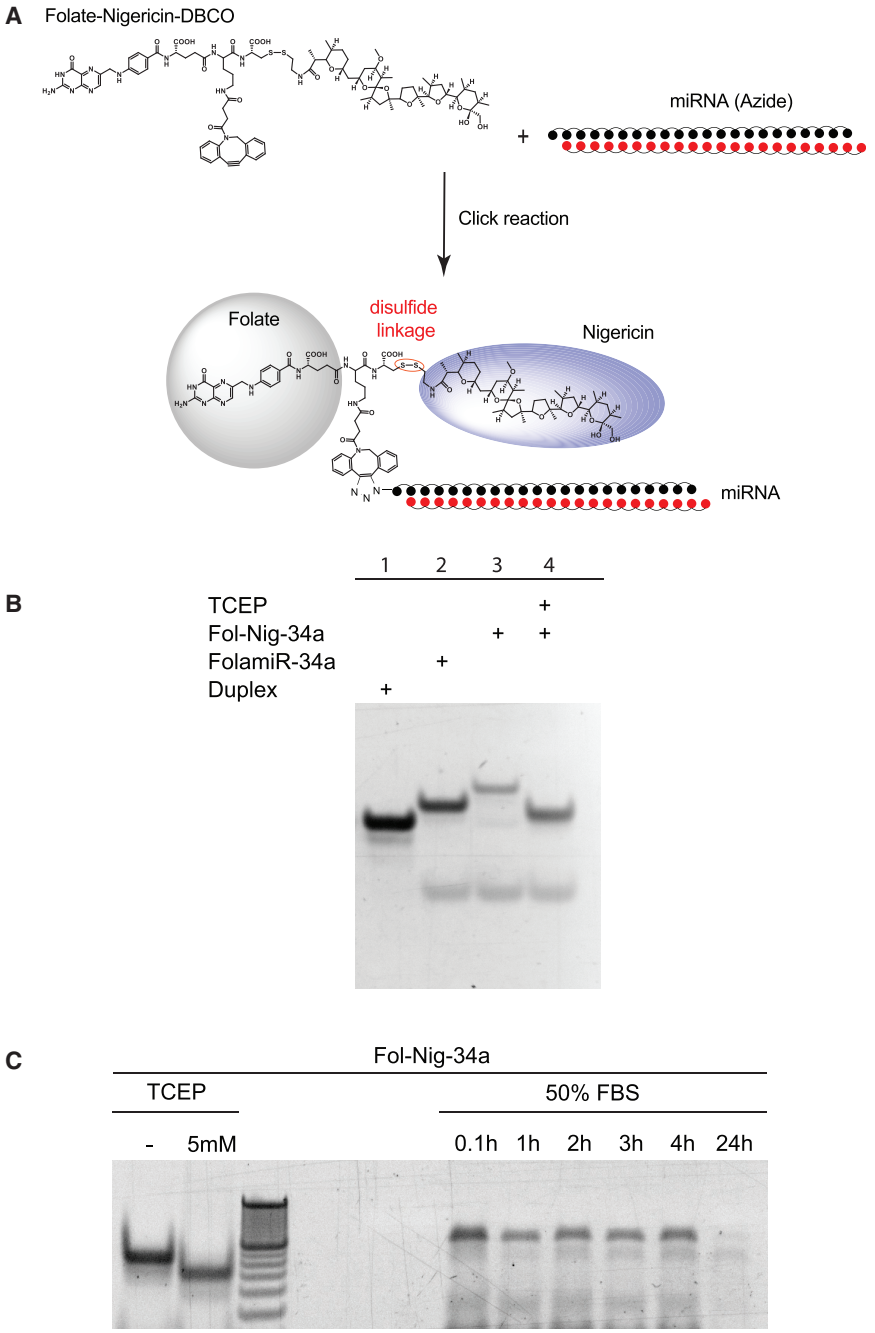

Figure 3. Evaluation of Folate-Nigericin-miRNA Conjugation and Stability in Serum

(A) Scheme of folate-nigericin-miR34a (Fol-Nig-34a) conjugation. (B) Gel-Red-stained polyacrylamide gel. Each lane was loaded with 200 pmol unconjugated oligo (Duplex) or folate miRNA. PAGE results suggested successful conjugation of folate-miRNA compounds, as visualized by the shift in mobility. The band shift in lane 4 indicates reduction of the disulfide bond between nigericin and folate miRNA. TCEP, reducing agent Tris (2-carboxyethyl)phosphine. (C) Gel-Red-stained polyacrylamide gel after resolution of folate-nigericin-miRNA after 50% serum exposure for different periods of time. TCEP (5 mM) is included as a positive control.

ligand-targeted delivery of nigericin promotes escape of cargo from entrapping endosomes.

Ligand-Targeted Delivery of Nigericin Promotes miR-34a Targeting, Cytosolic Distribution of miR-34a, and Engagement in the RISC

To validate that nigericin can mediate endosomal escape, we used a functional assay to monitor RNAi activity after delivery of miR-34a. Luciferase reporter assays were performed in MB-231 cells that express a sensor for miR-34a.[6] The *Renilla* level in these cells correlated inversely with miR-34a activity. These cell-based experiments indicated a rapid reduction in luciferase activity in Fol-Nig-34a-treated cells as soon as 18 h after treatment (reaching ~40% knockdown) and reaching 85% after 48 h (Figure 6A). This reduction in luciferase activity did not occur via gymnosis (Figure 6A, gray bars), nor was it observed in Fol-Nig-NC-treated cells, suggesting that the effect is specific to the presence of miR-34a and is not due to a side effect caused by potential nigericin-mediated toxicity. To eliminate that possibility, we conducted cellular toxicity assays, and the results showed that the first signs of toxicity related to nigericin compounds (folate-nigericin) were visualized at concentrations >1,000 nM (Figure 6B), well above the 50 nM concentration used for the functional assays. Next, we reasoned that, since the RISC programming is triggered by the appearance of double-stranded RNA in the cytosol (i.e., miRNA) and Argonaute (Ago) proteins localize diffusely in the cytosol and nucleus,[24,25] loading of miR-34a-5p into Ago would be indicative of cytosolic release. We first tested if miR-34a was enriched in the cytosol when cells were exposed to Fol-Nig-34a. Membrane-enclosed organelles and membrane-depleted (cytosolic) fractions were purified from post-nuclear supernatants (PNSs) obtained from homogenized cells. As shown in Figure 6C, cytosolic fractions were depleted of the endocytic marker EEA-1. miR-34a levels were measured in the resulting cytosolic fractions and were normalized to a ubiquitious cytosolic miRNA, miR-375. Treatment of cells with Fol-Nig-34a resulted in a 3.8-fold enrichment of miR-34a in the cytoplasm relative to Fola-miR-34a-treated cells (Figure 6C), suggesting that inclusion of nigericin promotes the endocytic release of miR-34a. To further test the

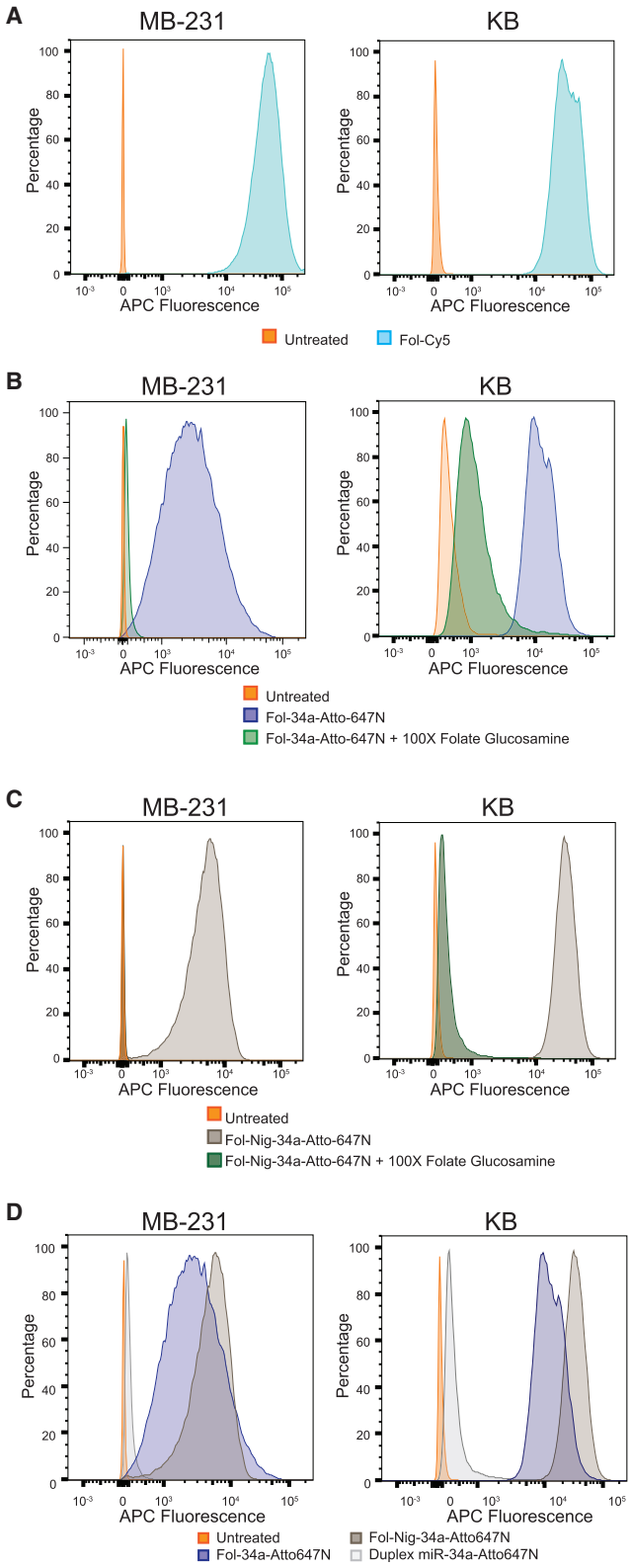

Figure 4. Folate-Nigericin-miRNA Conjugate Uptake Is Mediated by the Folate Receptor

(A) Confirmation of folate receptor expression in MB-231 breast cancer cells and in KB carcinoma cells. Histograms represent overlaid flow cytometry data as a percentage of unstained and folate-cyanate 5 (Fol-Cy5) cells. Displacement of Fol-34a-Atto647N (B) or Fol-Nig-34a-Atto647N (C) binding from MB-231 and KB cells (50 nM, 4°C) in the presence of 100-fold excess of folate-glucosamine conjugate. Histograms represent overlaid flow cytometry data as a percentage of unstained and Fol-34a-Atto647N- or Fol-Nig-34a-Atto647N-stained cells. (D) Folate-nigericin miRNA conjugate uptake is not mediated by gymnosis. MB-231 or KB cells were treated with Fol-34a-Atto647N, Fol-Nig-34a-Atto647N, or duplex miR-34a-Atto647N in the absence of transfection reagent. Histograms represent overlaid flow cytometry data as a percentage of unstained or Fol-34a-Atto647N-, Fol-Nig-34a-Atto647N-, or miR-34a-Atto647N-stained MB-231 and KB cells (50 nM, 4°C).

hypothesis that nigericin facilitates the release of RNA cargo into the cytoplasm, we performed RNA immunoprecipitation (RIP) assays by immunoprecipitating Ago proteins[26,27] in cells treated with FolamiR-34a or Fol-Nig-34a (Figure 6D). The results show that miRNA-34a-5p is more abundant in Ago RIP after folate-nigericin delivery (~6-fold) compared with delivery using the folate-only conjugation (Figure 6D, compare miR-34a qunatification: blue bar to red bar). Ago did not pull down RNU6B, as expected, but was associated with the positive control *let-7b*, validating the assay. To validate that binding of miR-34a to Ago was required for the miR-34a tumor-suppressive effect mediated by Fol-Nig-34a delivery, Ago2 was knocked down and cell proliferation was monitored (Figure 6E). The results show that Fol-Nig-34a only reduces cellular proliferation when Ago2 is present, indicating that Fol-Nig-34a cellular effects are mediated in part by the RNAi pathway. These results were also reproducible using a Fol-Nig-siRNA conjugate against Ras homolog gene family, member A (siRhoA), a known target that affects cell proliferation in MB-231 breast cancer cells[28] (Figure 6F). Taken together, these results support the hypothesis that a partial decrease in luciferase activity is RNAi-mediated and that the inclusion of nigericin in the folate carrier can help miR-34a escape from endosomes and become available in the cytosol to associate with Ago.

Inclusion of Nigericin in the Folate Carrier Enhances miRNA Activity

To test the hypothesis that the incorporation of nigericin in the folate carrier can lead to enhanced miR-34a activity in culture, time-response studies were conducted comparing FolamiR-34a and Fol-Nig-34a. The results show a difference in luciferase repression between FolamiR-34a (~30% reduction in *Renilla* activity) and Fol-Nig-34a (~85% reduction in *Renilla* activity, Figure 7A) that could indicate that FolamiR-34a gets entrapped inside endosomes by folate-targeted endocytosis. This could also explain why miR-34a delivered by folate alone is not abundant in Ago RIP (Figure 6D). Similarly, delivery of siRhoA by folate-nigericin results in higher antiproliferative activity compared with delivery using the folate-only carrier (Figure 7B).

To verify that the released miR-34a can repress endogenous targets, MB-231 cells were exposed to FolamiR-34a or Fol-Nig-34a and surface expression of PD-L1, a miR-34a target,[29] was monitored by

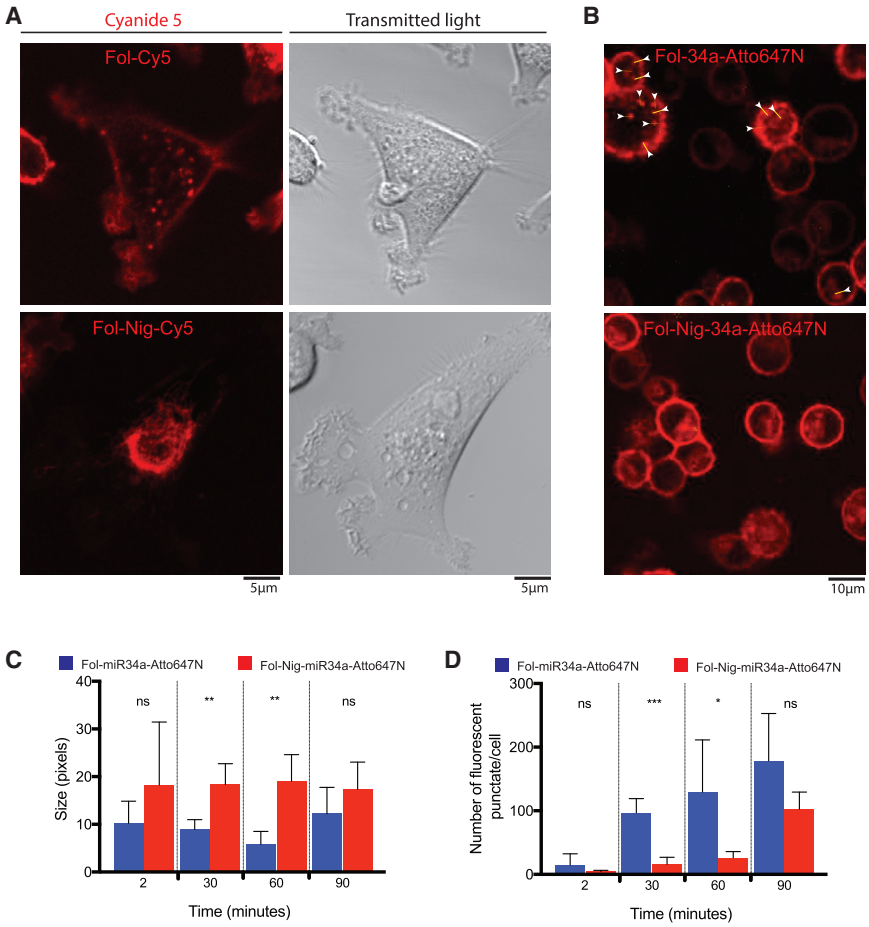

Figure 5. Ligand-Targeted Delivery of Nigericin Promotes Cargo Escape from Endosomes

(A) Representative confocal images of MB-231 cells treated with Fol-Cy5 or Fol-Nig-Cy5 (50 nM) at 15 min after treatment. (B) Representative confocal images of KB cells treated with Fol-34a-Atto647N or Fol-Nig-34a-Atto647N at 30 min after treatment. Comparison of fluorescent object size (C) and number (D) between Fol-34a-Atto647N- or Fol-Nig-34a-Atto647N-treated KB cells at different time points (n = 4; error bars, mean ± SD). Segmentation and quantification of subcellular vesicles was performed using the segmentation and quantification of subcellular shapes (Squassh) protocol.[33,34] Statistical analysis was performed with Student's t test (*$p < 0.05$, **$p < 0.01$, ***$p < 0.001$; ns, not significant).

flow cytometry. Only in the presence of Fol-Nig-34a was PD-L1 downregulated (Figure 7C). The effect observed was nearly identical to that observed following transfection with miR-34a mimics. Importantly, there was no reduction in PD-L1 in FR-negative (FR^-) A549 cells (Figure 7D), unless cells were transfected with miR-34a mimics, suggesting dependency of the FR on this response. This dependency was verified in MB-231 cells after treatment with excess folate-glucosamine, which mitigated the effect (Figure 7E). Nigericin inclusion also promoted miR-34a-dependent reductions in MET, an additional miR-34a target (Figure 7F).

Folate-miRNA Delivery Does Not Alter Endogenous miRNA Activity, nor Does It Result in Cytokine Release

To confirm that the folate-delivered miRNAs do not interfere with endogenous miRNA targeting, due to sequestering miRNA biogenesis or targeting machinery, the level of the miR-21 target PTEN was evaluated. Importantly, PTEN was not de-repressed in the presence of either miR-34a conjugate (Figure 7F). Using a more quantitative approach, it was determined that neither conjugate could alter *let-7* activity. Cells overexpressing a *let-7* reporter were treated with either FolamiR-34a or Fol-Nig-34a and sensor activity was monitored. In the absence of any treatment, a wild-type *let-7* sensor was reduced to ~85% of the activity obtained from a sensor with a mutated *let-7* targeting site (Figure 7G, left). This suggested that *let-7* levels were prominent in these cells and that any alterations in *let-7* targeting would be observed. Importantly, sensor activity remained consistent after treatment of cells with FolamiR-34a or Fol-Nig-34a (Figure 7G, right), suggesting that the miR-34a effect is specific and does not alter the targeting efficacy of other endogenous miRNAs.

Because exogenously delivered miRNAs have been met with unforeseeable negative events in the clinic due to immunostimulation, cytokine release in the presence of miR-34a conjugates was measured. Supernatants from human peripheral blood mononuclear cells (PBMCs) were harvested following their exposure to a high dose (100 nM) of folate-miR-34a conjugates and various cytokines levels were measured. Only the positive control, PBMCs treated with lipopolysaccharides (LPS) generated an increase in tumor necrosis factor alpha (TNF-α), interferon gamma (IFN-γ), and interleukin 6 (IL-6, Figure 8). There was no evidence of elevation of expression of any of the cytokines measured following 4 or 24 h of exposure of the cells to free nigericin, Fol-DBCO (the folate precursor), FolamiR-34a, or Fol-Nig-34a.

Taken together, these results support the hypothesis that rapid release of miRNA cargo from endosomal vesicles mediated by nigericin can improve miR-34a activity in culture.

DISCUSSION

Development of an effective delivery strategy for targeted, tissue-specific delivery of miRNAs is critical if the promise of miRNAs in the clinic is to be realized. Although the field of RNA medicine has had some recent breakthrough approvals with RNAi drugs, such as Onpattro (patisiran), which is targeted to the liver, advancement of miRNA-based therapeutics, specifically those for treating cancer

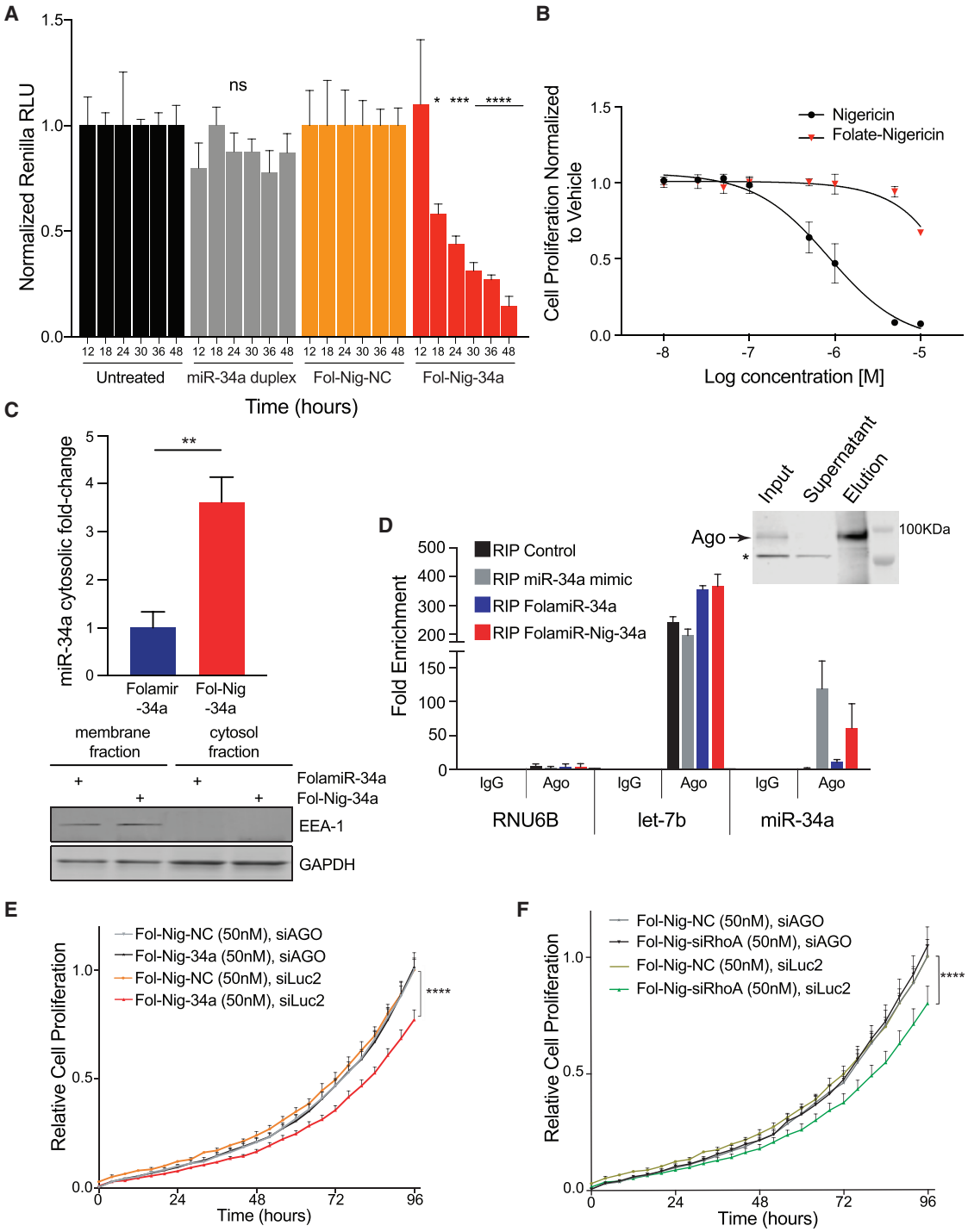

Figure 6. Nigericin Mediates Endosomal Escape of miRNA Cargo

(A) Effect of Fol-Nig-34a on miR-34a sensor silencing in cells in culture. Fol-Nig-34a data points were normalized to Fol-Nig-NC (negative control: scrambled miRNA). Nontransfected miR-34a duplex-treated cells were normalized to untreated cells. Each experiment corresponds to n = 3, four technical replicates per treatment, 50 nM; statistical analysis performed with one-way ANOVA and Bonferroni correction (*$p < 0.05$, ***$p < 0.001$, ****$p < 0.0001$; error bars: mean ± SD). (B) Effect of free nigericin and folate-nigericin on MB-231 cell growth. Data points were normalized to vehicle (DMSO). Error bars, mean ± SD; n = 6. (C) Accumulation of miR-34a in organelle-depleted cytosolic fraction after treatment with folate conjugates. miR-34a was measured via qRT-PCR from organelle-containing fractions, or organelle-depleted (cytosolic) fractions. Data are normalized to total cellular miR-34a. Western blots for the endocytic protein EEA-1 indicate that the cytosolic fractions were depleted of early endosomes. Statistical

(legend continued on next page)

lags behind. MiRagen is the only company that currently has a miRNA mimic in the clinic, miR-29a for the treatment or prevention of pathologic fibrosis (MRG-201). In this case MRG-201 is delivered topically to the eye (not yet in clinical trial) or is injected intradermally at the wound. Unfortunately, in the context of most cancers, systemic administration of the therapeutic is essential to reach not only the primary tumor but also any metastatic lesions. In this case, the delivered RNAs are subject to serum nucleases and are heavily diluted in circulation. To overcome these barriers, the affinity between the RNA and the target cell needs to be high, and the RNA needs to reach the target tissue rapidly and/or needs to be heavily protected in circulation. Two phase I studies were conducted delivering therapeutic miRNAs systemically within protective vehicles. The first, conducted by MiRNA Therapeutics delivered miR-34a mimics encapsulated within lipid nanoparticles, termed Smarticles that depend on the low pH of the tumor microenvironment for uptake.[30] Although efficacy was observed in some patients in the phase I trial, because of several severe immune-related toxic events, the trial was terminated early. The final findings of the study have yet to be published; however, toxicity can be attributed to either the vehicle or the miRNA. The second study that entered into phase I trial relied on epidermal-growth-factor-receptor (EGFR)-targeted minicells for delivery of miR-16 mimics.[31,32] TargomiRs, as they were named, succeeded in a phase I study, delivering a miRNA mimic inside of a protective vehicle. Although the trial showed promise, it still is not clear if the miR-16 mimic was actually delivered to the tumor site and if miR-16 targets were downregulated.[32] There is speculation that an immune-related response of TargomiRs may be responsible for the anti-tumor response that was due to the miRNA or the vehicle itself, as the vehicle was previously reported to contribute to immunologic effects in patients.[32] Regardless, the successful completion of the trial in 2017 is a benchmark in the miRNA therapeutics field. In the realm of miRNA mimic delivery, one thing can be agreed upon: eliminating the vehicle, reducing the overall concentration of the RNA being delivered, and/or modifying the RNA bases has the ability to overcome toxicity. Previously, we provided evidence of a novel way to deliver miRNAs free from a toxic delivery vehicle, and because of highly specific uptake into the tumor tissue, dosing was greatly reduced in comparison to other delivery vehicles, such as the Smarticle.[2,6] Herein, we have provided additional evidence that dosing can be even further reduced and efficacy increased if more of the miRNA can escape from the entrapped endosomes.

Vehicle-free delivery can be achieved with the use of small ligands. The addition of a ligand to a small RNA promotes its cellular uptake and trafficking, and although this is a key advantage in achieving the required specific biodistribution, it often suffers from a major limitation, endosomal entrapment. Upon binding to the membrane receptor, these ligands and the associated RNA cargo are internalized by receptor-mediated endocytosis and loaded into early endosomes. The contents of the endocytic vesicles are then sorted and trafficked intracellularly en route to the lysosome, which is where the nucleic acid cargo will be degraded or recycled back into the extracellular space. Recycling may account for the strong localization of FolamiRs to the plasma membrane in the absence of nigericin that we observed by confocal microscopy (Figure 2A). To avoid these therapeutically limiting effects, the ligand-RNA conjugates need to escape from the endosome into the cytoplasm where they can engage the RISC and modulate gene expression. Thus, the clinical application of small-RNA therapeutics requires the development of delivery strategies that not only direct tissue-specific internalization, but also effectively traffic the small RNA to the cytoplasm reaching biologically relevant doses.

Our previous research showed that it is possible to deliver a miRNA mimic to cancerous cells by simply conjugating the passenger strand to a folate ligand, with no signs of toxicity at the therapeutic dose tested.[6] Because folate conjugates are internalized via endocytosis, endosomal sequestration could be a limiting step in achieving significant clinical effects. We reasoned that the inclusion of an intramolecular endosomal escape mechanism could ensure robust cytosolic delivery of the RNA cargo and lead to enhanced miRNA activity. This approach relies on the use of a small molecule, nigericin, that upon cellular internalization gets cleaved from the folate carrier and localizes to the endosomal membrane, where it exchanges K^+ and water for an osmotically inactive proton (H^+), causing endosomal swelling.[18] To be effective, nigericin release has to occur in a controlled manner and only within the endosomes. Our preliminary evidence suggests that Fol-Nig-miRNA molecules are stable in 50% serum for at least 4 h, which, according to our previous observations, would be enough time for the conjugate to be internalized in the target cells.[6] Premature cleavage and release of nigericin in circulation is a concern, and further *in vivo* experiments are needed to evaluate this possibility.

The evidence presented here supports a new method of endosomal release of small RNAs that can be advantageous therapeutically. The aims of this strategy are to decrease the dosage of mimics needed to achieve effective gene modulation and minimize unwanted toxicity. The data support that ligand-targeted delivery of nigericin into endosomes can facilitate the escape of RNA cargo (e.g., miRNAs and siRNAs) from their entrapping endosomes, helping the small RNAs to become available in the cytoplasm, engage the RISC, and improve their RNAi activity. Thus, it is possible that with the help of nigericin, therapeutically relevant small RNAs could be delivered at low quantities and still show effective targeting.

analysis was performed with the two-tailed unpaired t test (n = 3; **$p < 0.01$; error bars: mean ± SD). (D) qRT-PCR results following Ago RIP from cells treated with FolamiR-34a or Fol-Nig-34a (100 nM). Transfected miR-34a mimic was used as the delivery control (6 nM). RNU6B, nontargeted control; *let-7b*, positive control. Experiments were repeated twice. Error bars, mean ± SD. Verification of Ago pulldown for Ago RIP experiments on right. *Nonspecific band. (E and F) Cell proliferation of MB-231 cells transfected with the indicated siRNA (siAGO or control, siLuc) and treated with the indicated folate-nigericin conjugate (E) Fol-Nig-34a and (F) Fol-Nig-siRhoA. Experiments were conducted in six replicates. Statistical analysis was performed with two-way ANOVA and Bonferroni correction (****$p < 0.0001$; error bars: mean ± SD).

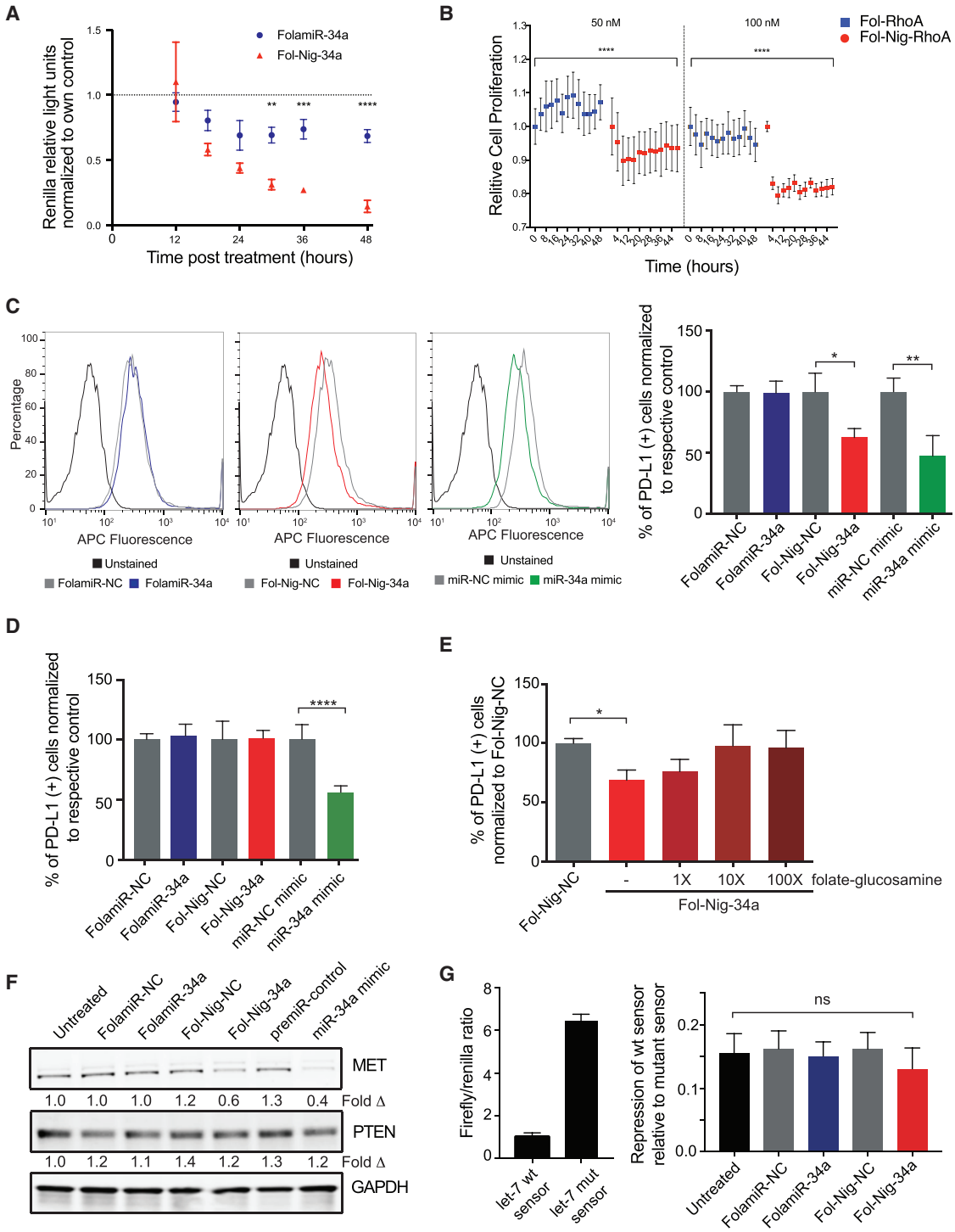

Figure 7. Incorporation of Nigericin into the Folate Carrier Enhances miRNA Activity *In Vitro*

(A) Targeted silencing of the miR-34a *Renilla* sensor using Fol-Nig-34a in cells in culture. Error bars, mean ± SD. Each experiment corresponds to n = 3; four technical replicates per treatment. (B) Effect of cellular proliferation in the presence of siRhoA conjugated to folate-only or folate-nigericin carrier. Statistical analysis performed with two-way ANOVA and Bonferroni correction (*p < 0.01, ***p < 0.001, ****p < 0.0001; error bars: mean ± SD). (C) Flow cytometry analysis of PD-L1 surface expression in FR^+ MB-231 cells treated with the indicated folate-conjugate (100 nM) or transfected with the same dose of the indicated miRNA mimics. Histograms represent overlaid flow cytometry data as a percentage of unstained and PD-L1-stained cells. Representative assay on the left. Quantified data from three biological replicates on the right. Error

(legend continued on next page)

We anticipate that, since nigericin is a small molecule that is nontoxic at the doses used and easy to conjugate to a small RNA using a variety of self-cleavable linkers, it will be easy to translate into the clinic. The challenge of the field of small-RNA delivery is to continue to design and optimize delivery mechanism at all stages, from the delivery process, to cytosolic release, to uptake into the RISC and mRNA cleavage, such that small RNAs can be delivered to the intended tissues at low effective doses in the absence of unwanted toxicity. There is scientific awareness of the potential of miRNA therapeutics, but with the lack of effective cytosolic release strategies, small-RNA therapeutics are predetermined to bottleneck in the clinic. Although these molecules have yet to reach *in vivo* experiments, the rigorous understanding of the safety and efficacy profiles of this new delivery and release platform could eventually enable the transition of ligand-RNA conjugates from the bench to the bedside.

MATERIALS AND METHODS

Cell Culture

MDA-MB-231 cells (MB-231 and HTB-26), KB carcinoma cells (CCL-17), and A549 lung epithelial carcinoma cells (CLL-185), mycoplasma-free, as determined by testing for mycoplasma contamination via the MycoAlert Mycoplasma Detection Kit (Lonza), were grown in RPMI 1640 medium with no folic acid (Life Technologies), supplemented with 10% fetal bovine serum (FBS; Sigma), penicillin (100 U/mL), and streptomycin (100 μg/mL) (HyClone, GE Healthcare Life Sciences), and maintained at 37°C in 5% CO_2. Authentication of MB-23, KB, and A549 cells was performed using short tandem repeat profiling (American Type Culture Collection [ATCC]).

Preparation of Pyridyldisulfide Amide, a Derivative of Nigericin

Folate-ethylenediamine (EDA), folate-Cys, and folate-dibenzocyclooctyne (DBCO) synthesis was performed as previously described.[6] Fol-Nig synthesis was performed as described in Rangasamy et al.[18] Nigericin-free acid (0.035 mmol), Py-SS-$(CH_2)_2NH_2$ (0.052 mmol), hexafluorophosphate azabenzotriazole tetramethyl uronium (HATU; 0.052 mmol), and N,N-diisopropylethylamine (DIPEA; 0.069 mmol) were dissolved in anhydrous CH_2Cl_2 (2.0 mL) and stirred under argon at room temperature overnight. The progress of the reaction was monitored by liquid chromatography–mass spectrometry (LC-MS). After complete conversion of the nigericin-free acid, the crude reaction mixture was subjected to purification by reverse-phase high-performance liquid chromatography (RP-HPLC; mobile phase A, 10 mM ammonium acetate, pH 7; organic phase B, acetonitrile; method: 0%–100% B in 35 min at 13 mL/min) and furnished nigericin-SS-amide derivative at a 55% yield, confirmed by LC-MS (mobile phase A, 10 mM ammonium bicarbonate, pH 7; organic phase B, acetonitrile; method: 0%–100% B in 15 min; retention time, 9.15 min; M + NH_4^+, 910.5).

Preparation of the Fol-Nig Conjugate

Fol-Nig synthesis was performed as previously described.[18] DIPEA was added dropwise to a stirred solution of folate-Cys (0.004 g, 0.007 mmol, 1.5 equiv) and pyridyldisulfide, an amide derivative of nigericin (0.004 g, 0.005 mmol, 1.0 equiv), in DMSO. The reaction mixture continued to be stirred at room temperature. The progress of the reaction was monitored by LC-MS. After complete conversion of Fol-Nig, the crude-reaction mixture was purified by RP-HPLC (mobile phase A, 10 mM ammonium acetate, pH 7; organic phase B, acetonitrile; method: 0%–40% B in 35 min at 13 mL/min) and furnished folate-nigericin at a 65% yield, confirmed by LC-MS (mobile phase A, 10 mM ammonium bicarbonate, pH 7; organic phase B, acetonitrile; method: 0%–100% B in 7 min; retention time, 4.0 min; M + H^+ = 1,440.0).

Preparation of Fol-Nig-DBCO

Folate-Nig-DBCO synthesis was performed as previously described.[18] DIPEA (0.0013 g, 0.010 mmol, 1.5 equiv) was added dropwise to a stirred solution of Fol-Nig (0.010 g, 0.0069 mmol, 1 equiv) and N-hydroxysuccinimide (NHS)-DBCO (0.003 g, 0.0076 mmol, 1.5 equiv) in DMSO. The reaction mixture was continuously stirred at room temperature. The progress of the reaction was monitored by LC-MS. After complete conversion of Fol-Nig-DBCO, the crude reaction mixture was purified by RP-HPLC (mobile phase A, 10 mM ammonium acetate, pH 7; organic phase B, acetonitrile; method: 0%–50% B in 35 min at 13 mL/min) and furnished Fol-Nig amide at a 65% yield, confirmed by LC-MS (mobile phase A, 10 mM ammonium bicarbonate, pH 7; organic phase B, acetonitrile; method: 0%–100% B in 12 min; retention time, 3.9 min; M + H^+ = 1,728.4).

Preparation of Fol-Nig-34a Conjugate

miRNA duplexes were constructed as previously described.[6] Briefly, a bi-orthogonal click reaction was performed between Fol-Nig-DBCO and the azide-modified antisense miR-34a (or scrambled miRNA). The click reaction was performed at a 1:10 molar ratio (azide oligo: Fol-Nig-DBCO) at room temperature in water for 8 h and then cooled to 4°C for 4 h. Unconjugated Fol-Nig-DBCO was removed from the reaction, using Oligo Clean and Concentrator (Zymo Research) per the manufacturer's instructions. Conjugation was verified by using

bars: mean ± SD. (D) Quantified flow cytometry data from three biological replicates of A549 cells treated with the indicated folate conjugate (100 nM) or transfected with the same dose of the indicated miRNA mimics. Error bars: mean ± SD. (E) Surface expression of PD-L1 was measured by flow cytometry after treatment of cells with Fol-Nig-34a in the presence or absence of excess competitor, folate-glucosamine. Expression after treatment with Fol-Nig-NC was included as a control (n = 3, three technical replicates per experiment; error bars: mean ± SD). (F) MB-231 cells were treated with the indicated conjugates or transfected with the indicated mimics. Lysates were obtained 48 h later and were resolved by SDS-PAGE. The following proteins were detected by immunoblot: MET, PTEN, and GAPDH. Fold change, normalized to GAPDH and relative to untreated is shown below the MET and PTEN blots. (G) MB-231 cells were transfected with either a wild-type (WT) or mutant *let-7* sensor. Relative firefly activity between the WT and mutant sensor are depicted on the left (n = 3; error bars: mean ± SD). Sensor expressing cells were treated with the indicated folate-conjugates. The effect of repression in the presence of folate conjugates is represented relative to a mutant sensor (n = 3; error bars: mean ± SD). Statistical analysis performed with one-way ANOVA and Bonferroni correction unless otherwise indicated (*$p < 0.1$, **$p < 0.01$, ***$p < 0.001$, ****$p < 0.0001$).

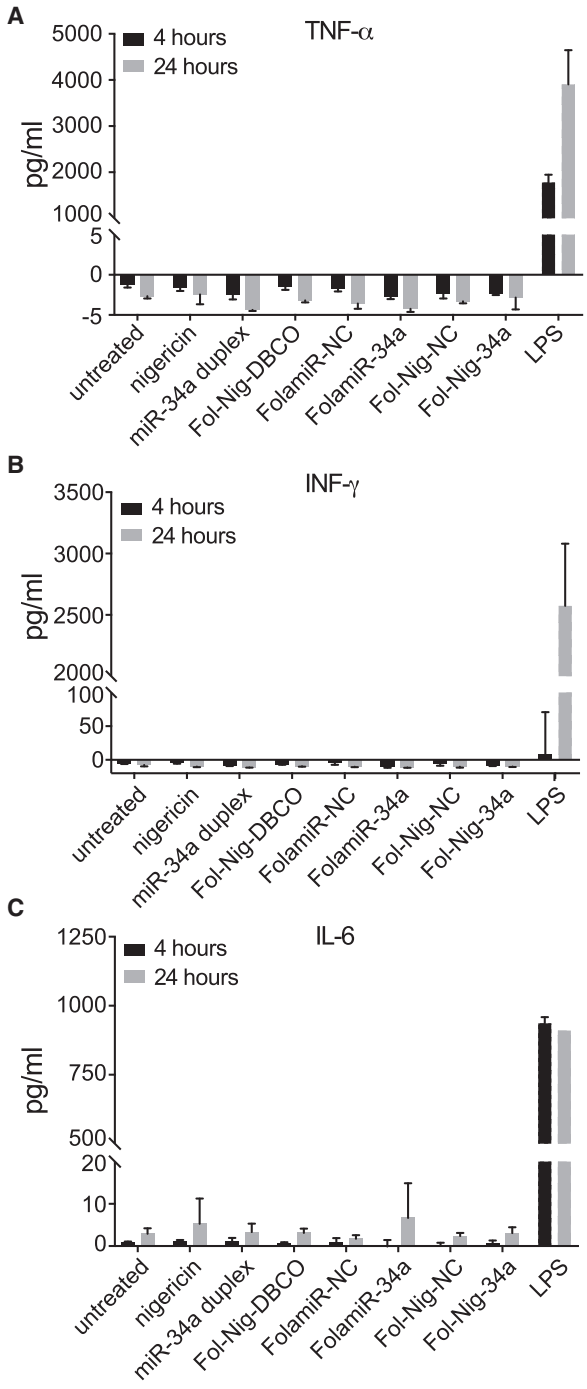

Figure 8. Innate Immune Response of Folate Conjugates in PBMCs

PBMCs were treated with 100 nM of the indicated molecules for either 4 or 24 h. Supernatants obtained were evaluated for the relevant cytokines: (A) tumor necrosis factor alpha (TNF-α), (B) interferon gamma (IFN-γ), and (C) interleukin 6 (IL-6). Supernatants from cells exposed to lipopolysaccharides (LPS) were included as the positive control. Statistical analysis was performed with one-way ANOVA and Bonferroni correction (n = 3; ns, not significant). Error bars: mean ± SD.

15% Tris-acetic acid-EDTA (TAE) native PAGE and MALDI spectral analysis. After conjugation, the miR-34a sense strand was annealed to the Fol-Nig-miR-34a antisense conjugate. Fol-Nig-DBCO-miR-34a antisense and miR-34a sense were mixed in an equal molar ratio (1:1, final concentration, 20 μM each) in annealing buffer: 10 mM Tris buffer, pH 7 (Sigma), supplemented with 50 mM NaCl (Sigma), and 1 mM EDTA (Sigma), and incubated at 95°C for 5 min; cooled slowly to room temperature; and then stored at −80°C. This compound is referred to as Fol-Nig-34a. For siRNA experiments, the previously reported oligonucleotides targeting the siRhoA gene[28] were used: sense 5′-GACAUGCUUGCUCAUAGUCTT-3′, antisense 3′-TTCUGUACGAACGAGUAUCAG-5′. For cellular uptake experiments, an Atto-647N fluorophore was attached to the 5′ end of the miR-34 antisense oligo and was used in the annealing step, generating the following compounds: Fol-34a-Atto647N and Fol-Nig-34a-Atto647N.

Stability Assay in Serum

Stability assays were performed as previously described.[6] Briefly, Fol-Nig-34a conjugates were incubated in 50% FBS (Sigma) in water at 37°C for the indicated times. RNA samples were collected and analyzed by using 15% TAE PAGE. The reducing agent TCEP was used as a positive control for nigericin reduction (5 mM, 20 min at room temperature).

Preparation of Fol-Cy5 Dye Conjugate

Fol-Cy5 synthesis was performed as previously described.[18] DIPEA (0.0004 g, 0.0032 mmol, 2 equiv) was added dropwise to a stirred solution of Fol-EDA (0.0008 g, 0.0016 mmol, 1 equiv) and NHS-Cy5 (0.001 g, 0.001 mmol, 1.1 equiv) in DMSO. The reaction mixture continued to be stirred at room temperature. The progress of the reaction was monitored by LC-MS. After complete conversion of Fol-Cy5, the crude reaction mixture was purified by RP-HPLC (mobile phase A: 10 mM ammonium acetate, pH 7; organic phase B: acetonitrile; method: 0%–50% B in 35 min at 13 mL/min) and furnished a Fol-Cy5 dye conjugate at a 85% yield, confirmed by LC-MS (mobile phase A: 10 mM ammonium bicarbonate, pH 7; organic phase B: acetonitrile; method: 0%–50% B in 12 min; retention time, 2.40 min; $M + H^+ = 949.2$).

Preparation of Fol-Nig-Cy5 Dye Conjugate

Fol-Nig-Cy5 synthesis was performed by adding DIPEA (0.0004 g, 0.0032 mmol, 2. equiv) dropwise to a stirred solution of Fol-Nig (0.0023 g, 0.0016 mmol, 1 equiv) and NHS-Cy5 (0.001 g, 0.0016 mmol, 1 equiv) in DMSO. The reaction mixture continued with stirring at room temperature. The progress of the reaction was monitored by LC-MS. After complete conversion of Fol-Nig-Cy5, the crude reaction mixture was purified by RP-HPLC (mobile phase A: 10 mM ammonium acetate, pH 7; organic phase B, acetonitrile; method: 0%–50% B in 35 min at 13 mL/min) and furnished Fol-Nig-Cy5 at a 65% yield, confirmed by LC-MS (mobile phase A: 10 mM ammonium bicarbonate, pH 7; organic phase B: acetonitrile; method: 0%–100% B in 12 min; retention time, 7.05 min; $M + H^+ = 1,906.0$).

Flow Cytometry

Flow cytometry was performed as described previously.[6] FR^+ human MB-231 cells, KB carcinoma cells, or FR^- A549 cells were detached by trypsinization, washed twice in ice-cold PBS (pH 7.4), and resuspended to a density of 1×10^7 cells/mL in serum-free medium (SFM). Cell viability was determined by trypan blue exclusion, and cells were used only if the viability was >80%. Next, flow cytometric analyses were performed according to standard protocols. The cell suspension (100 μL) was incubated with Fol-34a-Atto647N, Fol-Nig-34a-Atto647N, or Fol-Cy5 (50 nM) in the absence or presence of 10- to 100-fold molar excess of folate-glucosamine conjugate. For detection of PD-L1, cells were treated with the indicated folate conjugates, or transfected with miR-34a mimics, as described previously.[6] Forty-eight hours later, the cells were collected and incubated with a 1:100 dilution of anti-PD-L1 antibody (0.5 μL/50 μL cold PBS; 13684; Cell Signaling) for 1 h on ice. Unbound antibody was removed by washing the cells with ice-cold PBS. The cells were then incubated with 0.5 μL Alexa Fluro 647 secondary antibody (A-21244; Thermo Fisher) for detection. They were incubated at 4°C for 20 min, washed twice with ice-cold PBS, and analyzed by flow cytometry, using the LSR Fortessa flow cytometer (BD Biosciences, San Jose, CA, USA). Data were analyzed using FlowJo software v10 (Tree Star, Ashland, OR).

Live-Cell Imaging

Briefly, 8-well chambered slides with a glass coverslip bottom (Lab-TekTM Chambered Coverglass; Thermo Fisher Scientific, Denmark) were pre-treated with poly-D-lysine (0.1 mg/mL; Sigma-Aldrich) for 5 min, washed with PBS, and air-dried for 5 min. KB or MB-231 cells were plated onto prepared slides 1 day before the experiment at 2×10^4 cells/well and maintained in RPMI 1640 medium without folic acid (Life Technologies), supplemented with 10% FBS (Sigma), 100 U/mL penicillin, and 100 μg/mL streptomycin (Hyclone, GE Healthcare Life Sciences) at 37°C in 5% CO_2. For endosome co-localization studies, 1 μg plasmid encoding a GFP-Rab5b fusion protein (plasmid 61802; Addgene[21]) was transfected with Lipofectamine 2000 into MB-231 FR^+ cells, 24 h before the cells were harvested, and re-seeded into chambered slides. The slides were placed in a Nikon A1Rsi confocal microscope with a resonant scanner and piezo z-drive (Nikon Instruments Inc.) and a 20× objective Plan Apo 0.75 NA, equipped with a live imaging chamber (INU-TIZ-F1; Tokai Hit Corp., Japan), with temperature set to 37°C and continuous bubbling of 5% CO_2 in water. Image acquisition using NIS-elements software 4.5 (Nikon Instruments Inc., Japan) on a single focal plane was conducted for 3 h after addition of Fol-Cy5, Fol-Nig-Cy5, Fol-34a-Atto647N, and Fol-Nig-34a-Atto647N conjugates (50 nM). Images were further analyzed by using ImageJ 2.0.0 (NIH).

Segmentation and Quantification of Subcellular Vesicles

Segmentation and quantification of subcellular vesicles was performed with the segmentation and quantification of subcellular shapes (Squassh) protocol[33,34] in the Mosaic plugin in ImageJ V2.0 (NIH), using the following segmentation parameters: regularization, 0.1, and minimum object intensity, 0.160.

Live-Cell Proliferation Assay

MB-231 cells were transduced with 1% V/V NucLight Red Lentivirus (4476; Essen Bioscience), seeded on 96-well plates at 2,000 cells/well (3603; Corning), and incubated at 37°C with 5% CO_2 overnight. The next day, new medium containing different concentrations of the following reagents was added to the wells: vehicle (DMSO), nigericin, and Fol-Nig. The plate was placed in an IcuCyte S3 instrument (Essen Bioscience), and each well was imaged every 4 h for 24 h, using a standard-mode scan with a 10× objective and phase and red-filter acquisition. Each treatment consisted of three wells with five fields of view per well. Cell proliferation was quantified by counting the number of fluorescent nuclei over 24 h, using the Incucyte S3 Software (Essen Bioscience). Data were exported and analyzed, using GraphPad Prism v.7. Cell growth is represented as percentage of confluence relative to time 0. To determine the dose that causes growth inhibition of at least 50% (GI_{50}), the 24 h data points were selected and normalized to vehicle-treated cells.

Depletion of Membrane-Bound Vesicles and Cytoplasmic miR-34a Quantification

MB-231 cells (3×10^6) were seeded in a 10 cm plate. Twenty-four hours later, the cells were treated with 100 nM FolamiR-34a or Fol-Nig-34a for 18 h. Treated cells were homogenized, using a standard homogenization protocol.[35] In brief, cells were washed twice with ice-cold PBS (pH 7.4) and were scraped directly into PBS^+ solution (PBS containing 5 mM NaF and 0.5× protease inhibitors). The cells were centrifuged at 400 *g* for 5 min at 4°C. Supernatants were removed, and pelleted cells were homogenized by using a 25-gauge needle in 500 μL homogenization buffer (250 mM sucrose, 3 mM imidazole [pH 7.4], 1 mM EDTA, 0.03 mM cycloheximide, 1× protease inhibitors, and 1× phosphatase inhibitors). PNSs, containing cytosol and membrane fractions (mitochondria, Golgi, endosomes, and endoplasmic reticulum, among others) were collected by centrifugation at 2,000 *g* for 10 min at 4°C. To remove membrane-containing organelles, samples were fractionated by ultracentrifugation at 100,000 *g* for 1 h at 4°C. The supernatant was collected in a new 1.5 mL tube and centrifuged again at the same speed for another hour at 4°C, to further purify the cytosol fraction. RNA was isolated from the resulting cytosolic fractions using Qiazol reagent (QIAGEN) followed by ethanol precipitation. RT was performed using the miRscript II RT kit (QIAGEN) with HiFlex buffer. Real-time PCR was conducted using miScript SYBR Green PCR Kit (QIAGEN) with the following primers: miR-375 (non-target RNA, MiScript primer assay; QIAGEN), and mir-34a-5p (MiScript primer assay; QIAGEN). Real-time PCR data were analyzed using the $2^{-\Delta\Delta Ct}$ method and expressed as fold enrichment.

RNA Immunoprecipitation Assay

RNA precipitation assays were performed as previously described.[26,27] Briefly, MB-231 cells transfected with a miR-34a mimic were used as the control. MB-231 cells (7×10^5 cells/well) were seeded into 6-well plates and maintained overnight in RPMI 1640 medium with no folic acid (Life Technologies), supplemented with 10% FBS (Sigma), 100 U/mL penicillin, and 100 μg/mL

streptomycin (Hyclone, GE Healthcare Life Sciences) at 37°C in 5% CO_2. The next day, medium was replaced with 800 μL of fresh complete medium. Transfection of miR-34a mimic (final concentration, 6 nM; Ambion) was performed with Lipofectamine RNAimax (Life Technologies) by mixing 100 μL SFM containing mir-34a mimic (Ambion) and 100 μL SFM with 7.5 μL Lipofectamine RNAimax (Life Technologies), incubated at room temperature for 5 min, and then added to the wells. The cells were incubated for 4 h at 37°C in 5% CO_2, and the medium was replaced with 2 mL of fresh complete medium. For FolamiR-34a or Fol-Nig-34a treatments, MB-231 cells (8×10^5 cells/well) in complete medium were seeded into 6-well plates containing FolamiR-34a or Fol-Nig-34a diluted in 1 mL SFM (RPMI) to a final concentration of 100 nM. After 24 h, the cells were put on ice, washed twice with ice-cold PBS, and immersed in 1 mL PBS. Cells were cross-linked at 400 mJ/cm^2 and then again at 200 mJ/cm^2 in a UV cross-linker (XL-1000; SpectroLinker). Cells were scraped directly into lysis buffer (1× PBS, 1% vol/vol NP40 substitute, 0.5% wt/vol sodium deoxycholate, and 0.1% wt/vol SDS). Next, the lysates were centrifuged in a prechilled tabletop ultracentrifuge at 21,000 *g* for 20 min at 4°C. Cleared lysates were incubated with Dynabead Protein A beads (Life Technologies) prepared with 2A8 anti-Ago[26,36] (MABE56; Millipore) or normal mouse IgG (12-371; Millipore) for 90 min at 4°C, washed, and resuspended, as previously described.[26] RNA was isolated using Qiazol reagent (QIAGEN) followed by ethanol precipitation. RT was performed using the miRscript II RT kit (QIAGEN) with HiSpec buffer. Real-time PCR was conducted using miScript SYBR Green PCR Kit (QIAGEN) with the following primers: RNU6B (non-target RNA, MiScript primer assay; QIAGEN), *let-7b-1* (positive control, MiScript primer assay; QIAGEN), and mir-34a (MiScript primer assay; QIAGEN). Real-time PCR data were analyzed using the $2^{-\Delta\Delta Ct}$ method[37,38] and expressed as fold enrichment.

Ago2 Knockdown

GeneSolution siRNAs (1027416; QIAGEN) were used to knockdown Ago2, according to the manufacturer's instructions. Briefly, MB-231 cells were transfected with 25 pmol siRNAs using 7.5 μL Lipofectamine RNAimax (Life Technologies) in 6 wells (80% confluence). Protein knockdown was measured after 48 h. siLuc2 was used as a negative control.

Protein Isolation and Western Blotting

MB-231 cells were collected in RNAlater (Life Technologies) and stored at −80°C. Frozen cells were placed in 2 mL collection tubes containing radioimmunoprecipitation assay buffer (1× PBS, 1% NP-40, 0.5% sodium deoxycholate, 0.1% SDS, and 1× protease inhibitor). Cells were incubated for 10 min on ice and centrifuged for 10 min at 4°C (20,000 *g*), supernatant was collected, and 50 μg protein was resolved on 12% TGX gels (Bio-Rad) and transferred to polyvinylidene difluoride (PVDF) membranes. The Revert Total Protein Staining kit (Li-Cor) was used as the protein loading control, according to the manufacturer's instructions. The following primary antibodies were used for detection: 2A8 anti-Ago (1:1,000, MABE56; Millipore), anti-MET (1:1,000, 4560; Cell Signaling), anti-PTEN (1:1,000, 9559; Cell Signaling), anti-EEA-1 (1:1,000, 2411; Cell Signaling), and anti-GAPDH (1:1,000, 2118; Cell Signaling). Protein detection was performed after incubation with secondary antibodies (Li-Cor), membranes were washed, and signal was acquired using Li-Cor Odyssey CLX (Li-Cor).

Cytokine Analysis

Cell culture supernatants from human peripheral blood mononuclear cells [(PBMCs) American Type Culture Collection (ATCC)] treated with 100 nM folate conjugates were used to test for the production of cytokines, tumor necrosis factor alpha (TNF-α), interferon gamma (IFN-γ), and interleukin-6 (IL-6) concentrations using ELISA Max Deluxe Kit (Biolegand), according to the manufacturer's instructions. Briefly, 2×10^5 PBMCs seeded into a 96-well plate were treated with 100 nM folate conjugates. Cell culture supernatants were collected at 4 and 24 h after treatment. One day prior to the assay, the respective capture antibodies were coated onto 96-well plates. The following day, all samples and standards were added to the plate and incubated for 2 h at room temperature. Supernatants were removed, and the wells were washed. Detection antibody was added, and the plates were incubated for 1 h at room temperature. The wells were washed again and incubated with Avidin-horseradish peroxidase solution for 30 min at room temperature. After a final wash, substrate solution was added, and the plates were incubated for 15 min at room temperature. Stop solution was added, and absorbance data were acquired at 450 and 560 nm using a GloMax plate reader (Promega). The 560 nm reading was subtracted from the 450 nm reading. Cytokine standard curves were used to calculate the cytokine concentrations (pg/mL) in the cell culture supernatant. Cell culture supernatants from LPS (0.2 mg/mL)-treated PBMCs were used as positive controls.

AUTHOR CONTRIBUTIONS

E.A.O., P.S.L., and A.L.K. designed the study. E.A.O., A.M.A., S.T., L.R., S.M., P.S.L., and A.L.K. analyzed the data. E.A.O. and A.L.K. wrote the manuscript. E.A.O., A.M.A, and A.L.K. edited the manuscript. E.A.O. performed the confocal imaging, stability assays, uptake and specificity analysis, toxicity assessment, and Ago IP and knockdown studies. A.M.A. performed chloroquine experiments, fractionation experiments, and PD-L1 and MET miR-34a target analysis. S.M. performed PBMC studies. Folate-nigericin-DBCO synthesis was performed by L.R and S.T. A.L.K. and P.S.L. conceived and supervised the project.

CONFLICTS OF INTEREST

A.L.K. and P.S.L. are inventors on PCT U.S. patent application 67538-02 submitted by Purdue University, which covers methods and uses of targeted delivery of miRNAs and endosomal escape. P.S.L. owns shares in Endocyte, which develops small-molecule drug conjugates using the folate-targeting technology discussed in the article. The remaining authors declare no competing interests.

ACKNOWLEDGMENTS

This work was supported by the National Institutes of Health, United States grants R01 CA226259 and R01 CA205420 (A.L.K.). E.A.O. is a

recipient of a Fulbright Award from Ecuador. A.M.A. was supported by an Andrew's Fellowship, Purdue University, United States. GFP-Rab5 was a gift from Gia Voeltz (Addgene plasmid 61802).

REFERENCES

1. Kasinski, A.L., Kelnar, K., Stahlhut, C., Orellana, E., Zhao, J., Shimer, E., Dysart, S., Chen, X., Bader, A.G., and Slack, F.J. (2015). A combinatorial microRNA therapeutics approach to suppressing non-small cell lung cancer. Oncogene *34*, 3547–3555.
2. Kasinski, A.L., and Slack, F.J. (2012). miRNA-34 prevents cancer initiation and progression in a therapeutically resistant K-ras and p53-induced mouse model of lung adenocarcinoma. Cancer Res. *72*, 5576–5587.
3. Kasinski, A.L., and Slack, F.J. (2011). Epigenetics and genetics. MicroRNAs en route to the clinic: progress in validating and targeting microRNAs for cancer therapy. Nat. Rev. Cancer *11*, 849–864.
4. Zuckerman, J.E., Gritli, I., Tolcher, A., Heidel, J.D., Lim, D., Morgan, R., Chmielowski, B., Ribas, A., Davis, M.E., and Yen, Y. (2014). Correlating animal and human phase Ia/Ib clinical data with CALAA-01, a targeted, polymer-based nanoparticle containing siRNA. Proc. Natl. Acad. Sci. USA *111*, 11449–11454.
5. Wang, H., Jiang, Y., Peng, H., Chen, Y., Zhu, P., and Huang, Y. (2015). Recent progress in microRNA delivery for cancer therapy by non-viral synthetic vectors. Adv. Drug Deliv. Rev. *81*, 142–160.
6. Orellana, E.A., Tenneti, S., Rangasamy, L., Lyle, L.T., Low, P.S., and Kasinski, A.L. (2017). FolamiRs: Ligand-targeted, vehicle-free delivery of microRNAs for the treatment of cancer. Sci. Transl. Med. *9*, eaam9327.
7. Orellana, E.A., and Kasinski, A.L. (2017). No vehicle, no problem. Oncotarget *8*, 96470–96471.
8. Shete, H.K., Prabhu, R.H., and Patravale, V.B. (2014). Endosomal escape: a bottleneck in intracellular delivery. J. Nanosci. Nanotechnol. *14*, 460–474.
9. Vlashi, E., Kelderhouse, L.E., Sturgis, J.E., and Low, P.S. (2013). Effect of folate-targeted nanoparticle size on their rates of penetration into solid tumors. ACS Nano *7*, 8573–8582.
10. Yang, J., Chen, H., Vlahov, I.R., Cheng, J.-X., and Low, P.S. (2006). Evaluation of disulfide reduction during receptor-mediated endocytosis by using FRET imaging. Proc. Natl. Acad. Sci. USA *103*, 13872–13877.
11. Yang, J., Chen, H., Vlahov, I.R., Cheng, J.-X., and Low, P.S. (2007). Characterization of the pH of folate receptor-containing endosomes and the rate of hydrolysis of internalized acid-labile folate-drug conjugates. J. Pharmacol. Exp. Ther. *321*, 462–468.
12. Varkouhi, A.K., Scholte, M., Storm, G., and Haisma, H.J. (2011). Endosomal escape pathways for delivery of biologicals. J. Control. Release *151*, 220–228.
13. Lundberg, P., El-Andaloussi, S., Sütlü, T., Johansson, H., and Langel, U. (2007). Delivery of short interfering RNA using endosomolytic cell-penetrating peptides. FASEB J. *21*, 2664–2671.
14. Oliveira, S., van Rooy, I., Kranenburg, O., Storm, G., and Schiffelers, R.M. (2007). Fusogenic peptides enhance endosomal escape improving siRNA-induced silencing of oncogenes. Int. J. Pharm. *331*, 211–214.
15. Erazo-Oliveras, A., Muthukrishnan, N., Baker, R., Wang, T.-Y., and Pellois, J.-P. (2012). Improving the endosomal escape of cell-penetrating peptides and their cargos: strategies and challenges. Pharmaceuticals (Basel) *5*, 1177–1209.
16. Behr, J.-P. (1997). The proton sponge: A trick to enter cells the viruses did not exploit. CHIMIA Int. J. Chem. *51*, 34–36.
17. Oliveira, S., Fretz, M.M., Høgset, A., Storm, G., and Schiffelers, R.M. (2007). Photochemical internalization enhances silencing of epidermal growth factor receptor through improved endosomal escape of siRNA. Biochim. Biophys. Acta *1768*, 1211–1217.
18. Rangasamy, L., Chelvam, V., Kanduluru, A.K., Srinivasarao, M., Bandara, N.A., You, F., Orellana, E.A., Kasinski, A.L., and Low, P.S. (2018). New Mechanism for Release of Endosomal Contents: Osmotic Lysis via Nigericin-Mediated K^+/H^+ Exchange. Bioconjug. Chem. *29*, 1047–1059.
19. Steinrauf, L.K., Pinkerton, M., and Chamberlin, J.W. (1968). The structure of nigericin. Biochem. Biophys. Res. Commun. *33*, 29–31.
20. Graven, S.N., Estrada-O, S., and Lardy, H.A. (1966). Alkali metal cation release and respiratory inhibition induced by nigericin in rat liver mitochondria. Proc. Natl. Acad. Sci. USA *56*, 654–658.
21. Rowland, A.A., Chitwood, P.J., Phillips, M.J., and Voeltz, G.K. (2014). ER contact sites define the position and timing of endosome fission. Cell *159*, 1027–1041.
22. Marks, I.S., Kang, J.S., Jones, B.T., Landmark, K.J., Cleland, A.J., and Taton, T.A. (2011). Strain-promoted "click" chemistry for terminal labeling of DNA. Bioconjug. Chem. *22*, 1259–1263.
23. Parker, N., Turk, M.J., Westrick, E., Lewis, J.D., Low, P.S., and Leamon, C.P. (2005). Folate receptor expression in carcinomas and normal tissues determined by a quantitative radioligand binding assay. Anal. Biochem. *338*, 284–293.
24. Liu, J., Valencia-Sanchez, M.A., Hannon, G.J., and Parker, R. (2005). MicroRNA-dependent localization of targeted mRNAs to mammalian P-bodies. Nat. Cell Biol. *7*, 719–723.
25. Leung, A.K.L., Calabrese, J.M., and Sharp, P.A. (2006). Quantitative analysis of Argonaute protein reveals microRNA-dependent localization to stress granules. Proc. Natl. Acad. Sci. USA *103*, 18125–18130.
26. Moore, M.J., Zhang, C., Gantman, E.C., Mele, A., Darnell, J.C., and Darnell, R.B. (2014). Mapping Argonaute and conventional RNA-binding protein interactions with RNA at single-nucleotide resolution using HITS-CLIP and CIMS analysis. Nat. Protoc. *9*, 263–293.
27. Moore, M.J., Scheel, T.K.H., Luna, J.M., Park, C.Y., Fak, J.J., Nishiuchi, E., Rice, C.M., and Darnell, R.B. (2015). miRNA-target chimeras reveal miRNA 3′-end pairing as a major determinant of Argonaute target specificity. Nat. Commun. *6*, 8864.
28. Sun, H.-W., Tong, S.-L., He, J., Wang, Q., Zou, L., Ma, S.-J., Tan, H.Y., Luo, J.F., and Wu, H.X. (2007). RhoA and RhoC -siRNA inhibit the proliferation and invasiveness activity of human gastric carcinoma by Rho/PI3K/Akt pathway. World J. Gastroenterol. *13*, 3517–3522.
29. Wang, X., Li, J., Dong, K., Lin, F., Long, M., Ouyang, Y., Wei, J., Chen, X., Weng, Y., He, T., and Zhang, H. (2015). Tumor suppressor miR-34a targets PD-L1 and functions as a potential immunotherapeutic target in acute myeloid leukemia. Cell. Signal. *27*, 443–452.
30. Beg, M.S., Brenner, A.J., Sachdev, J., Borad, M., Kang, Y.-K., Stoudemire, J., Smith, S., Bader, A.G., Kim, S., and Hong, D.S. (2017). Phase I study of MRX34, a liposomal miR-34a mimic, administered twice weekly in patients with advanced solid tumors. Invest. New Drugs *35*, 180–188.
31. Viteri, S., and Rosell, R. (2018). An innovative mesothelioma treatment based on miR-16 mimic loaded EGFR targeted minicells (TargomiRs). Transl. Lung Cancer Res. *7* (*Suppl 1*), S1–S4.
32. van Zandwijk, N., Pavlakis, N., Kao, S.C., Linton, A., Boyer, M.J., Clarke, S., Huynh, Y., Chrzanowska, A., Fulham, M.J., Bailey, D.L., et al. (2017). Safety and activity of microRNA-loaded minicells in patients with recurrent malignant pleural mesothelioma: a first-in-man, phase 1, open-label, dose-escalation study. Lancet Oncol. *18*, 1386–1396.
33. Paul, G., Cardinale, J., and Sbalzarini, I.F. (2013). Coupling image restoration and segmentation: A generalized linear model/bregman perspective. Int. J. Comput. Vis. *104*, 69–93.
34. Rizk, A., Paul, G., Incardona, P., Bugarski, M., Mansouri, M., Niemann, A., Ziegler, U., Berger, P., and Sbalzarini, I.F. (2014). Segmentation and quantification of subcellular structures in fluorescence microscopy images using Squassh. Nat. Protoc. *9*, 586–596.
35. de Araújo, M.E.G., Lamberti, G., and Huber, L.A. (2015). Homogenization of Mammalian Cells. Cold Spring Harb. Protoc. *2015*, 1009–1012.
36. Nelson, P.T., De Planell-Saguer, M., Lamprinaki, S., Kiriakidou, M., Zhang, P., O'Doherty, U., and Mourelatos, Z. (2007). A novel monoclonal antibody against human Argonaute proteins reveals unexpected characteristics of miRNAs in human blood cells. RNA *13*, 1787–1792.
37. Livak, K.J., and Schmittgen, T.D. (2001). Analysis of relative gene expression data using real-time quantitative PCR and the 2(-Δ Δ C(T)) Method. Methods *25*, 402–408.
38. Yuan, J.S., Reed, A., Chen, F., and Stewart, C.N., Jr. (2006). Statistical analysis of real-time PCR data. BMC Bioinformatics *7*, 85.